LA-UR- 09-00194

*Approved for public release; distribution is unlimited.*

*Title:* Temperature measurements of partially-melted tin as a function of shock pressure

*Author(s):* A. Seifter, M. R. Furlanetto, M. Grover, D. B. Holtkamp, A. W. Obst, J. R. Payton, J. B. Stone, G. D. Stevens, D. C. Swift, L. J. Tabaka, W. D. Turley, L. R. Veeser

*Intended for:* Journal of Applied Physics

THE PAPER SUBMITTED FOR A LA-UR-# IS BASED ON THE EARLIER VERSION OF THIS PAPER (WITH THE LA-UR-08-06420)

Los Alamos NATIONAL LABORATORY EST. 1943



Form 836 (7/06)

# Temperature measurements of partially-melted tin as a function of shock pressure

A. Seifter[1], M. R. Furlanetto[2], M. Grover[3], D. B. Holtkamp[2], G. Macrum[3], A.W. Obst[2], J.R. Payton[2], J. B. Stone[2], G. D. Stevens[3], D. C. Swift[4], L. J. Tabaka[2], W. D. Turley[3], and L. R. Veeser[3]

[1] *Los Alamos National Laboratory (LANL), Accelerator Operations and Technology Division (ABS), MS H817, Los Alamos, NM. USA*

[2] *LANL, Physics Division (P-23), MS H803, Los Alamos, NM. USA*

[3] *National Securities Technologies, Goleta, CA. USA*

[4] *Lawrence Livermore National Laboratory, Livermore, CA. USA*

(Dated: January 8, 2009)

Equilibrium equation of state theory predicts that the free surface release temperature of shock loaded tin will show a plateau of 505 K in the pressure range from 19.5 to 33.0 GPa, corresponding to the solid-liquid mixed-phase region. In this paper we report free surface temperature measurements on shock-loaded tin from 15 to 31 GPa using multi-wavelength optical pyrometry. The shock waves were generated by direct contact of detonating high explosive with the sample. The pressure in the sample was determined by free surface velocity measurements using Photon Doppler Velocimetry. The emitted thermal radiance was measured at four wavelength bands in the near IR region from 1.5 to 5.0 $\mu$m. The samples in most of the experiments had diamond-turned surface finishes, with a few samples being polished or ball rolled. At pressures higher than 25 GPa the measured free surface temperatures were higher than the predicted 505 K and increased with increasing pressure. This deviation could be explained by hot spots and/or variations in surface emissivity and requires a further investigation.

## I. INTRODUCTION

Temperature is one of three parameters (besides pressure and volume) necessary for describing a thermodynamically complete equation-of-state (EOS). The development of a complete EOS is more complicated in the case when the material subject to dynamic loading undergoes phase transitions on compression or release. For the purposes of this study, the liquid phase of tin can be reached either directly by shock loading to pressures higher than 50 GPa or on release from shock pressures above 33 GPa. Since melt pressures for shock or release are easily accessible with various experimental techniques (gas or powder guns, high explosive (HE) driven flyer plates, direct HE drive and laser ablation), shock-melted tin has been well studied experimentally over the recent decades [1–6].

Since tin is non-toxic and easy to work with it is a good material for the investigation of phase changes. It is predicted by theory (and will be discussed in the next section) that the free surface release temperature of tin shocked in the pressure range between 19.5 and 33.0 GPa is the ambient pressure melting temperature of 505 K. The calculated temperature does not rise above 505 K in this pressure range because energy added to the metal is expended in melting process and is not predicted to rise until all of the tin is melted. In the past, temperature measurements by means of optical pyrometry have been subject to doubt because this technique is based on several assumptions which are not always well justified [7]. These assumptions include a spatially uniform surface temperature (no hot spots) and emissivity, no contamination of the measured signals by background light, and no surface or interface effects, such as thermal conductivity or localized plastic work, which would substantively alter the measured temperature. The observation of a constant and reproducible free-surface temperature for a shock loaded sample over a significant range of Hugoniot pressures would render it possible to test the applicability of pyrometry to free-surface shock-physics experiments and to determine its accuracy, independent of EOS and plastic work parameters used to calculate the expected temperature. This development would also make it possible to check techniques for determining the dynamic spectral emissivity without the involvement of reference techniques, such as Neutron Resonance Spectroscopy [8] or Raman Spectroscopy [9].

## II. THEORETICAL BACKGROUND: SN PHASE DIAGRAM

The equilibrium phase diagram of tin in the range from 0 to 50 GPa and 0 to 2500 K is shown in figure 1 [10, 11]. At ambient pressure, tin adopts the $\beta$-phase (ct(4)) between 291 K and 505 K, above 505 K it is in the liquid-phase. The $\alpha$-phase (fcc(8)) below 291 K is not relevant for this study, and is not shown. At room temperature the phase-transition from the $\beta$ to $\gamma$ phase occurs around

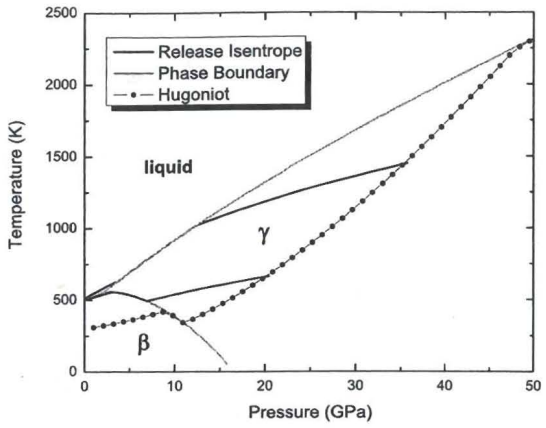


FIG. 1: Tin phase diagram [10]

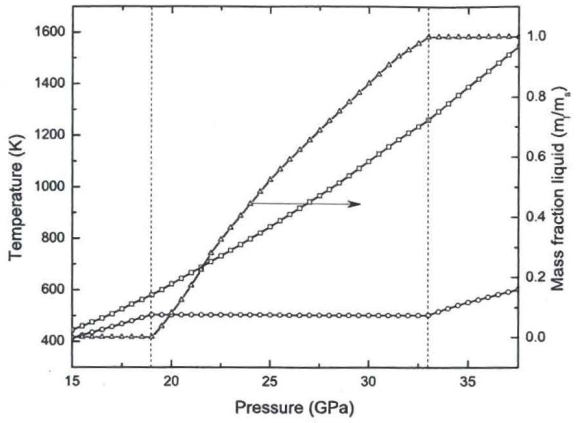


FIG. 2: The calculated Hugoniot temperature (squares), the free surface temperature (circles) and the mass fraction of liquid after release to ambient pressure (triangles) as function of Hugoniot pressure [14]

9.2 GPa [12]. With increasing pressure, the melting-point of tin increases and at 2.9 GPa and a temperature of 581 K tin reaches a triple point ($\beta$, $\gamma$ and liquid phase) [13].

The principal Hugoniot, the locus of points that can be reached by a single shock, is shown as the curve farthest to the right in figure 1. The release isentropes from this curve are shallower. Consequently melt on release can occur at lower pressures and temperatures than melt on compression. At the onset of melt on release, at a Hugoniot pressure of 19.5 GPa, the release intersects the $\beta$-$\gamma$ phase boundary at 7 GPa and then follows first the $\beta$-$\gamma$ phase boundary from 7 GPa to the triple point and then the melt curve to the ambient-pressure melting temperature of 505 K. At 33 GPa, the lowest Hugoniot pressure for complete melt on release, the release intersects the melt curve at 12 GPa and from there follows the melt curve through the triple point to 505 K.

The principal Hugoniot intersects the $\beta$-$\gamma$ phase boundary at a pressure of about 8.5 GPa and a temperature of 435 K, and follows the phase boundary to a pressure of 10.9 GPa and a temperature of 344 K. At a pressure of about 48 GPa the principal Hugoniot intersects the melt-curve slightly above 2200 K and follows it to a pressure of 57 GPa at a temperature of 2507 K from whence it departs entirely into the liquid phase at higher pressures.

The calculated Hugoniot temperature, free surface temperature and mass-fraction of liquid in the material released to ambient pressure are shown in figure 2 as a function of Hugoniot pressure. The mass-fraction of liquid upon release to ambient pressure increases from 0 at a Hugoniot pressure of 19.5 GPa to 1 at 33.0 GPa. For Hugoniot pressures below 19.5 GPa the sample never reaches the liquid phase; for pressures above 33.0 GPa the release isentrope leaves the melt curve before ambient pressure is reached, resulting in a totally molten sample at ambient pressure with a temperature above 505 K.

The phase-diagram shown in figure 1, as well as the free-surface temperature, Hugoniot temperature, andmass-fraction of liquid Sn shown in figure 2 were calculated assuming thermal and pressure equilibrium between the phases. The effect of plastic work on compression and release has been ignored; the flow stress of tin (at least in the beta phase) is small enough [15] that it is reasonable to ignore such contributions [16].

## III. EXPERIMENTAL SETUP

The experiments were performed at the Special Technology Laboratory (STL) in Santa Barbara, CA, using an HE containment vessel, which is designed to perform small-scale shock physics experiments in a laboratory environment and is certified for a total amount of HE up to 10 g TNT equivalent [17]. Figure 3 shows the experimental setup enclosed by the containment vessel.

The thermally emitted light from the sample is collimated with an off-axis-parabolic mirror (OAP) and relayed through the chamber window (a sandwich made of $CaF_2$ and Sapphire windows) to the outside of thecontainment vessel. The aluminum vacuum chamber, using a thin $CaF_2$ window, is used to achieve pressures in the milliTorr range to prevent shock-induced airglow. A dichroic beamsplitter (DBS; a short pass filter with a cutoff wavelength of approximately 1000 nm) reflects the long wavelength IR light onto another OAP which focuses the light into a 1 mm diameter chalcogenide IR (C2) fiber [17] for transport to the IR pyrometer. The thermally-emitted light with wavelengths less than 1000

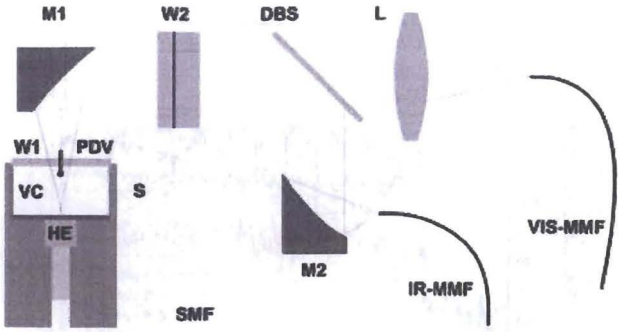


FIG. 3: The experimental setup. S, sample; HE, high explosive; VC, aluminum vacuum chamber; W1, $CaF_2$ window; PDV, Photon Doppler Velocimetry probe; M1, ø 25 mm (f/2) off axis parabolic mirror; W2, $CaF_2$ - $Al_2O_3$ sandwich chamber window; DBS, dichroic beamsplitter; M2, ø 25 mm (f/1) off axis parabolic mirror; L, ø 25 mm (f/2) lens; IR-MMF, infrared multimode fiber to pyrometer; VIS-MMF, visible multimode fiber to photo multiplier tube; SMF, single-mode fiber to PDV system.

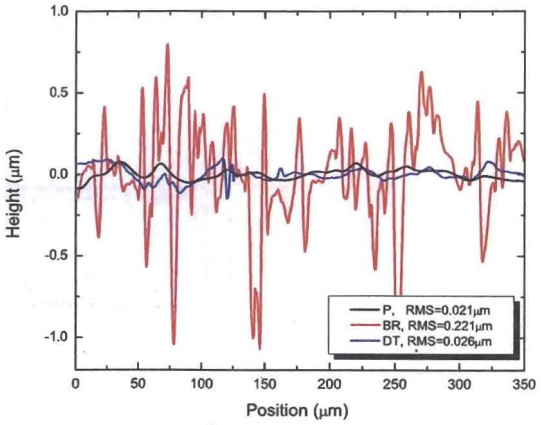


FIG. 4: (Color online) Surface roughness of the three different methods of sample preparation: polished (P), ball-rolling (BR), and diamond-turning (DT).

nm is transmitted through the DBS and focused with a single lens (ø 25 mm, f/2) into a 1 mm diameter, low-OH visible fiber. The fiber transports the light to a photo multiplier tube (PMT) to monitor unwanted background light. The incoming light at the IR pyrometer is collimated using a ZnSe lens and then spectrally split with three DBS. The bandwiths are narrowed using bandpass filters and the light is focused by ZnSe lenses onto four liquid-nitrogen cooled InSb detectors. The rise-time of these detectors is below 20 ns, and they are very linear and sensitive to low light levels. These characteristics permits measurement of radiance temperatures [39]as low as 400 K with a time resolution of less than 50ns. For more details on the design, calibration and performance of the IR pyrometer see references [18, 19]. A small hole (ø 1.0 mm) was drilled in the CaF2 vacuum chamber window and the PDV probe (a small fiber collimator on a single-mode fiber) was glued into this hole to measure the free-surface velocity averaged over a ø 0.3 mm spot at the center of the sample. The obstruction of the optical path of the pyrometer by the PDV probe was taken into account during the calibration of the pyrometer system. For more details on the measurement of velocities by means of PDV see reference 20. For more details on the experimental setup see reference 6.

The tin samples had a diameter of 40 mm and a thickness between 1.5 and 3.5 mm. An HE pellet with a diameter of 12.7 mm and thickness of 12 mm was press-fit to one face of the sample and ignited by an RP-80 EBW detonator [21]. The side of the tin samples in contact with the HE had a 16 $\mu$-inch (0.4 $\mu$m) machine finish; the side facing the diagnostics was either diamond-turned (mirror like with machining marks visible under a magnifying glass), ball-rolled, or polished. Figure 4 shows the interferometric surface roughness measurements for a diamond-turned, a ball-rolled, and a polished samples in . For a detailed description of the process of ball-rolling and the expected benefits (suppressing the production of ejecta by compacting the surface) see references 6, 22, 23. The sample material was purchased from ESPI metals [24] as a ø 50.4 mm rod with a purity of 99.999+ %. The samples had elongated grains with lengths of up to 15 mm and widths of up to 2 mm. Machining of the samples (including diamond turning) was performed at the Material Science and Technology (MST) division of the Los Alamos National Laboratory.

The shock wave transmitted by HE in direct contact with the sample is an unsupported (i.e. "Taylor") wave [25] and decays as it passes through the sample. This hydrodynamic behavior was used to change the pressures by using samples of different thickness. If the sample is too thick, edge effects perturb the stress profile experienced by the sample. For this study approximately one-dimensional loading conditions were desired accros the region sampled by the IR measurements and the velocimeter, limiting the range of pressures accessible with a given HE type. To increase the accessible pressure range, two different HE materials were used, namely Detasheet [26] for lower pressures and the more energetic PBX 9501 [27] for pressures above 22 GPa. The expected pressures from 1-D and 2-D simulations [28–30] are shown for various sample thicknesses in figure 5 in the next section, and compared with the Hugoniot pressures inferred experimentally.

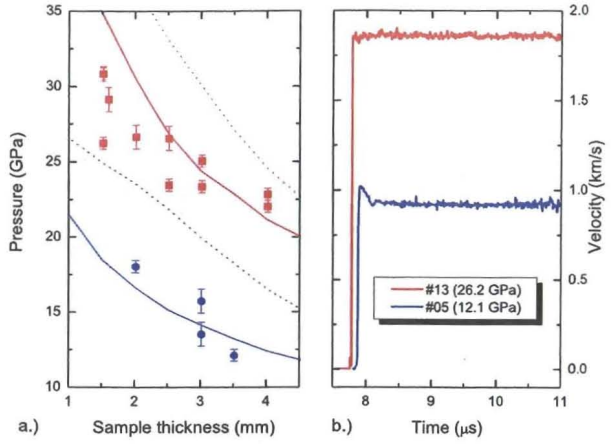


FIG. 5: (Color online) (a) Inferred and calculated Hugoniot pressures as function of sample thickness (blue dots: measured pressures for detasheet, blue full line: calculated pressure for detasheet assuming a ø 1.4 mm detonator, blue dotted line: calculated pressure for detasheet assuming a ø 5.0 mm detonator, red squares: measured pressures for PBX9501, red full line: calculated pressure for PBX9501 assuming a ø 3.0 mm detonator, red dotted line: calculated pressure for PBX9501 assuming a ø 5.0 mm detonator) and (b) free-surface velocity versus time for experiments #05 and #13.

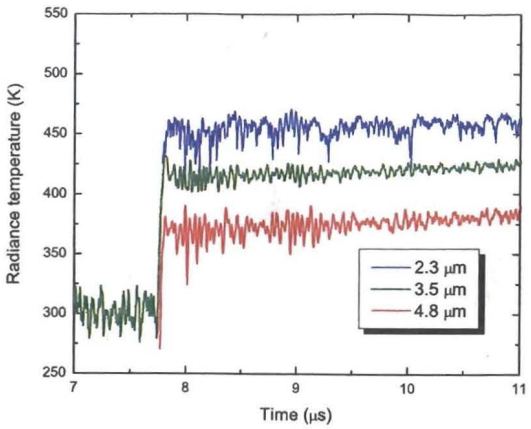


FIG. 6: (Color online) Radiance temperatures for 3 channels of the IR pyrometer for experiment #07 (23.4 GPa).

## IV. RESULTS

Sixteen experiments were performed. A summary of the HE used, the sample thickness and surface finish, the pressure inferred from the surface velocity, and the measured temperatures is given in table I.

Figure 5a shows the achieved Hugoniot pressures for all experiments as well as the expected pressure [40] as a function of sample thickness for both types of HE used. A pressure around 20 GPa could not be achieved by using either Detasheet with a very thin sample or PBX 9501 with a very thick sample. It can be seen that the pressure can be predicted fairly well but there is a large variability on the achieved pressure, which we think can be related to the way the experimental package was assembled and how the HE was mated to the sample[41]. The free-surface velocities as a function of time for experiments #05 and 13 are shown in figure 5b. At about 7.75 $\mu$s after detonation time the shock front reaches the free surface. For experiment #05 (26.2 GPa) the free surface velocity stays constant (within the noise) for more than 4 $\mu$s. No pullback was observed after the shock breakout because the sample is more than 50 % (mass) liquid and does not have much strength[42]. For experiment #13 (12.1 GPa) a pullback signal can be clearly seen. After this pullback the free surface velocity stays constant, probably indicating spallation of the sample [31].

The radiance temperatures for three channels as a function of time for experiment #07 are shown in figure 6. Since the dynamic normal spectral emissivities as a function of wavelength and temperature are not known, a lower and upper limit for the normal spectral emissivity was assumed for each channel. This assumption results in a lower and upper limit for the true temperature. If these emissivity estimates are reasonable and no unwanted background light occurs, then the sample temperature must be less than the smallest true-temperature upper limit and larger than the smallest lower limit to be consistent with all three data channels. For more information on this method of analyzing pyrometry date see references 18, 32–34.

Above the melt boundary, the temperatures extracted from experiments performed on samples with polished surfaces are slightly higher (10 K to 60 K) than for diamond-turned samples in the same pressure range. For ball rolled samples the temperature differential is between 100 K to 130 K higher. (see table I). Although the same free-surface temperatures were measured for both ball-rolled and diamond-turned samples at 18 GPa [6], we think that in the mixed-phase region (Hugoniot pressures between 19.5 and 33 GPa) the surface roughness of a ball-rolled sample causes more temperature non-uniformities (e.g. hot spots) than for a diamond-turned surface. The higher post-shock temperatures measured on polished samples are believed to be caused by either some polishing material embedded in the surface of the sample or by tiny scratches, which give raise to a minute amount of ejecta and surface work.

The post-shock, free-surface temperatures for all experiments on diamond-turned samples (and on one ball-rolled and one polished surface below 19.5 GPa) are shown in figure 7. The error bars represent the upper and lower limits of the overlapping region of the true

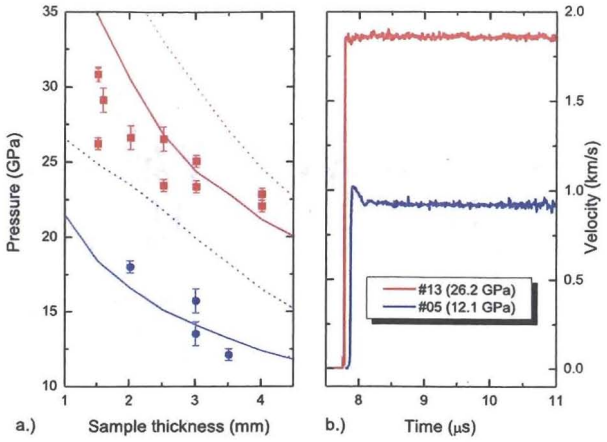


FIG. 5: (Color online) (a) Inferred and calculated Hugoniot pressures as function of sample thickness (blue dots: measured pressures for detasheet, blue full line: calculated pressure for detasheet assuming a ø 1.4 mm detonator, blue dotted line: calculated pressure for detasheet assuming a ø 5.0 mm detonator, red squares: measured pressures for PBX9501, red full line: calculated pressure for PBX9501 assuming a ø 3.0 mm detonator, red dotted line: calculated pressure for PBX9501 assuming a ø 5.0 mm detonator) and (b) free-surface velocity versus time for experiments #05 and #13.

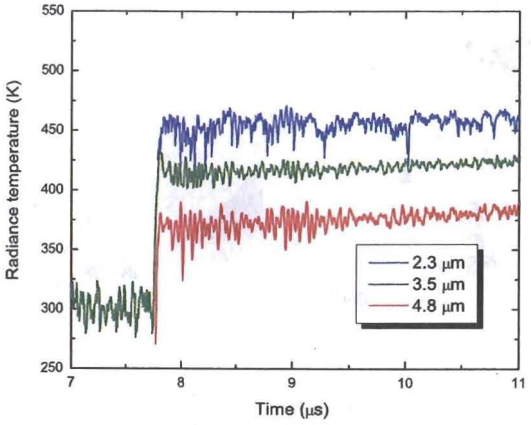


FIG. 6: (Color online) Radiance temperatures for 3 channels of the IR pyrometer for experiment #07 (23.4 GPa).

## IV. RESULTS

Sixteen experiments were performed. A summary of the HE used, the sample thickness and surface finish, the pressure inferred from the surface velocity, and the measured temperatures is given in table I.

Figure 5a shows the achieved Hugoniot pressures for all experiments as well as the expected pressure[40] as a function of sample thickness for both types of HE used. A pressure around 20 GPa could not be achieved by using either Detasheet with a very thin sample or PBX 9501 with a very thick sample. It can be seen that the pressure can be predicted fairly well but there is a large variability on the achieved pressure, which we think can be related to the way the experimental package was assembled and how the HE was mated to the sample[41]. The free-surface velocities as a function of time for experiments #05 and 13 are shown in figure 5b. At about 7.75 $\mu$s after detonation time the shock front reaches the free surface. For experiment #05 (26.2 GPa) the free surface velocity stays constant (within the noise) for more than 4 $\mu$s. No pullback was observed after the shock breakout because the sample is more than 50 % (mass) liquid and does not have much strength[42]. For experiment #13 (12.1 GPa) a pullback signal can be clearly seen. After this pullback the free surface velocity stays constant, probably indicating spallation of the sample [31].

The radiance temperatures for three channels as a function of time for experiment #07 are shown in figure 6. Since the dynamic normal spectral emissivities as a function of wavelength and temperature are not known, a lower and upper limit for the normal spectral emissivity was assumed for each channel. This assumption results in a lower and upper limit for the true temperature. If these emissivity estimates are reasonable and no unwanted background light occurs, then the sample temperature must be less than the smallest true-temperature upper limit and larger than the smallest lower limit to be consistent with all three data channels. For more information on this method of analyzing pyrometry date see references 18, 32–34.

Above the melt boundary, the temperatures extracted from experiments performed on samples with polished surfaces are slightly higher (10 K to 60 K) than for diamond-turned samples in the same pressure range. For ball rolled samples the temperature differential is between 100 K to 130 K higher. (see table I). Although the same free-surface temperatures were measured for both ball-rolled and diamond-turned samples at 18 GPa [6], we think that in the mixed-phase region (Hugoniot pressures between 19.5 and 33 GPa) the surface roughness of a ball-rolled sample causes more temperature non-uniformities (e.g. hot spots) than for a diamond-turned surface. The higher post-shock temperatures measured on polished samples are believed to be caused by either some polishing material embedded in the surface of the sample or by tiny scratches, which give raise to a minute amount of ejecta and surface work.

The post-shock, free-surface temperatures for all experiments on diamond-turned samples (and on one ball-rolled and one polished surface below 19.5 GPa) are shown in figure 7. The error bars represent the upper and lower limits of the overlapping region of the true

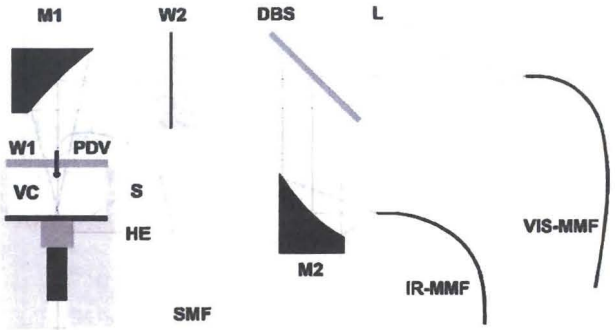


FIG. 3: The experimental setup. S, sample; HE, high explosive; VC, aluminum vacuum chamber; W1, $CaF_2$ window; PDV, Photon Doppler Velocimetry probe; M1, ø 25 mm (f/2) off axis parabolic mirror; W2, $CaF_2$ - $Al_2O_3$ sandwich chamber window; DBS, dichroic beamsplitter; M2, ø 25 mm (f/1) off axis parabolic mirror; L, ø 25 mm (f/2) lens; IR-MMF, infrared multimode fiber to pyrometer; VIS-MMF, visible multimode fiber to photo multiplier tube; SMF, single-mode fiber to PDV system.

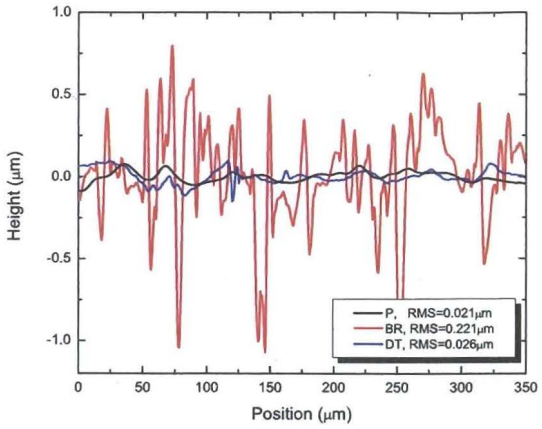


FIG. 4: (Color online) Surface roughness of the three different methods of sample preparation: polished (P), ball-rolling (BR), and diamond-turning (DT).

nm is transmitted through the DBS and focused with a single lens (ø 25 mm, f/2) into a 1 mm diameter, low-OH visible fiber. The fiber transports the light to a photo multiplier tube (PMT) to monitor unwanted background light. The incoming light at the IR pyrometer is collimated using a ZnSe lens and then spectrally split with three DBS. The bandwiths are narrowed using bandpass filters and the light is focused by ZnSe lenses onto four liquid-nitrogen cooled InSb detectors. The rise-time of these detectors is below 20 ns, and they are very linear and sensitive to low light levels. These characteristics permits measurement of radiance temperatures [39]as low as 400 K with a time resolution of less than 50ns. For more details on the design, calibration and performance of the IR pyrometer see references [18, 19]. A small hole (ø 1.0 mm) was drilled in the CaF2 vacuum chamber window and the PDV probe (a small fiber collimator on a single-mode fiber) was glued into this hole to measure the free-surface velocity averaged over a ø 0.3 mm spot at the center of the sample. The obstruction of the optical path of the pyrometer by the PDV probe was taken into account during the calibration of the pyrometer system. For more details on the measurement of velocities by means of PDV see reference 20. For more details on the experimental setup see reference 6.

The tin samples had a diameter of 40 mm and a thickness between 1.5 and 3.5 mm. An HE pellet with a diameter of 12.7 mm and thickness of 12 mm was press-fit to one face of the sample and ignited by an RP-80 EBW detonator [21]. The side of the tin samples in contact with the HE had a 16 $\mu$-inch (0.4 $\mu$m) machine finish; the side facing the diagnostics was either diamond-turned (mirror like with machining marks visible under a magnifying glass), ball-rolled, or polished. Figure 4 shows the interferometric surface roughness measurements for a diamond-turned, a ball-rolled, and a polished samples in . For a detailed description of the process of ball-rolling and the expected benefits (suppressing the production of ejecta by compacting the surface) see references 6, 22, 23. The sample material was purchased from ESPI metals [24] as a ø 50.4 mm rod with a purity of 99.999+ %. The samples had elongated grains with lengths of up to 15 mm and widths of up to 2 mm. Machining of the samples (including diamond turning) was performed at the Material Science and Technology (MST) division of the Los Alamos National Laboratory.

The shock wave transmitted by HE in direct contact with the sample is an unsupported (i.e. "Taylor") wave [25] and decays as it passes through the sample. This hydrodynamic behavior was used to change the pressures by using samples of different thickness. If the sample is too thick, edge effects perturb the stress profile experienced by the sample. For this study approximately one-dimensional loading conditions were desired accros the region sampled by the IR measurements and the velocimeter, limiting the range of pressures accessible with a given HE type. To increase the accessible pressure range, two different HE materials were used, namely Detasheet [26] for lower pressures and the more energetic PBX 9501 [27] for pressures above 22 GPa. The expected pressures from 1-D and 2-D simulations [28–30] are shown for various sample thicknesses in figure 5 in the next section, and compared with the Hugoniot pressures inferred experimentally.

TABLE I: Type of HE (DS, Detasheet; 9501, PBX 9501), sample thickness, surface finish of the samples, achieved Hugoniot pressure, and measured temperature for all experiments.

| Experiment # | HE | Thickness (mm) | Surface finish | Pressure (GPa) | Temperature (K)[a] |
|---|---|---|---|---|---|
| 01 | DS | 2.0 | DT | 18.0±0.8 | 470±25 |
| 02 | 9501 | 4.0 | DT | 22.0±0.4 | 490±30 |
| 03 | 9501 | 4.0 | BR | 22.8±0.4 | 620±25 |
| 04 | 9501 | 1.5 | DT | 30.8±0.4 | 565±25 |
| 05 | 9501 | 1.5 | BR | 26.2±0.8 | 650±35 |
| 06 | 9501 | 3.0 | DT | 23.3±0.4 | 490±25 |
| 07 | 9501 | 2.5 | DT | 23.4±0.4 | 500±25 |
| 08 | 9501 | 1.5 | BR | 29.1±0.4 | 675±25 |
| 09 | 9501 | 2.0 | DT | 26.6±0.4 | 550±25 |
| 10 | DS | 3.0 | DT | 25.7±0.8 | N.A. |
| 11 | 9501 | 1.5 | P | 30.8±0.4 | 625±25 |
| 12 | 9501 | 3.0 | P | 25.0±0.4 | 560±40 |
| 13 | DS | 3.0 | DT | 12.1±0.4 | 360±40 |
| 14 | 9501 | 2.5 | DT | 26.5±0.4 | 530±35 |
| 15 | DS | 3.0 | P | 13.5±0.8 | 390±55 |
| 16 | 9501 | 1.0 Cu + 1.5 Sn | DT | 22.8±0.4 | 500±40 |

[a]Temperature as obtained by hi-low method [18]; no correction for temperature reading due to hot spots was applied.

temperature bands of the individual channels. Below 25 GPa, the measured temperatures are in good agreement with the predicted free-surface temperatures. Above 25 GPa (#04, 09 and 14) the measured temperatures are considerably higher than the calculated temperature of 505 K. Only for experiment #14 (26.5 GPa) does the error bar reach the expected temperature of 505 K. The expected plateau of 505 K between the Hugoniot pressure of 19.5 and 33.0 GPa could not be observed; within their error bars, all data points are consistent with a straight line sloping upward from lower to higher temperatures.

The measured true temperature values for one experiment below 25 GPa (#06: $p_H$ = 23.3 GPa) and one experiment above 25 GPa (#09: $p_H$ = 26.6 GPa) are shown in figure 8 for all wavelengths for which a signal was obtained. The measured true temperature for experiment #09 increases with decreasing wavelength. This is a strong indication that the thermal radiance is spatially non-uniform, i.e., the surface likely has hot-spots [35].

This change of behavior in the pressure region around 25 GPa was also observed in experiments measuring the amount of ejecta as a function of pressure at the same experimental facility (STL) for Sn samples made of the same material (ESPI) and with the same surface preparation [2]. In these experiments the amount of ejecta increased by a factor of ~10 above about 22.0 GPa. We do not yet have an explanation for this increase in the amount of ejecta and appearance of hot-spots. In yet another study, a dramatic change in the tin free surface

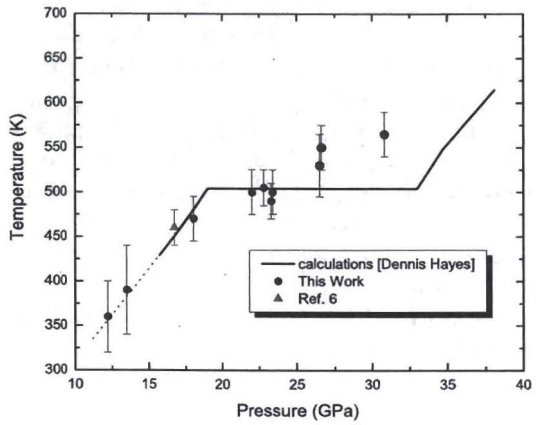


FIG. 7: (Color online) Measured temperatures (points) as a function of Hugoniot pressure, as well as expected free-surface temperature (line) [14].

reflectivity from highly specular to diffuse was observed at the shock-induced solid-liquid phase boundary. This result could signal significant changes in surface emisivity and may partially explain the observed variations [36]. The appearance of hot-spots above 22 GPa in free-surface temperature measurements on shock-loaded tin is also supported by IR-imaging experiments performed at STL [4, 5].

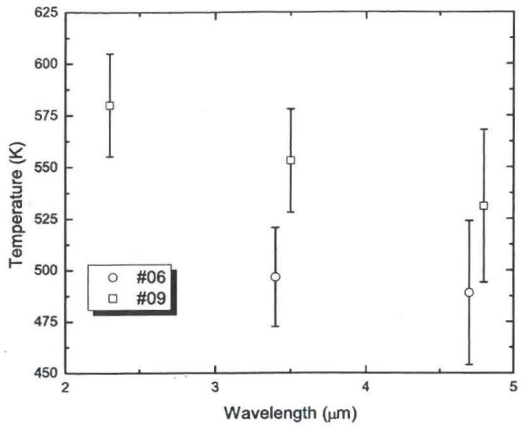


FIG. 8: True temperature for individual channels in experiments #06 and 09 (Hugoniot pressures 23.3±4 and 26.6±4 GPa) (wavelength for #06 shifted by 0.1 m for clarity of the graph).

In free-surface temperature measurements on surfaces with a non-uniform temperature distribution, the shorter-wavelength measurements are more sensitive to the hotter regions. The longer wavelength channels show less dependence on the hot-spots but have larger errorbars because the uncertainty in the normal spectral emissivity is larger for longer wavelengths. Therefore, a better understanding of the surface temperature between the hot spots can be obtained if the shorter wavelengths are ignored. If we use only the longest wavelengths for experiments #04, 09 and 14, then all error bars reach the expected 505 K. However, the longer wavelength channels have a rather high uncertainty in temperature (see fig. 8) and thus these results are not accurate enough to confirm whether or not there is a plateau in the free surface temperature at 505 K in the pressure range between 19.5 and 33.0 GPa.

## V. CONCLUSIONS

A series of experiments at the STL Boom Box facility was performed to look for a plateau at 505 K in the free-surface temperature of shock-loaded tin in the Hugoniot pressure range between 19.5 and 33.0 GPa. Samples with a polished or ball-rolled surface finish exhibited temperatures between 10 to 130 K higher than samples with a diamond-turned surface, and may be explained by increased emissivity or temperature non-uniformity.

An increase of the free surface temperature with increasing Hugoniot pressure was observed in accordance with theoretical predictions for pressures below 20 GPa. In four experiments (#02, 06, 07 and 16) in the pressure range between 22.0 and 23.4 GPa the measured free surface temperature was very close to 505 K. Unfortunately, a Hugoniot pressure near the onset of the predicted plateau (19.5 GPa) could not be achieved with the HE systems available (see figure 5a). At Hugoniot pressures higher than 25 GPa, the measured free-surface temperatures again increased with increasing pressure. We believe that these temperatures are higher because of spatial temperature and/or emissivity non-uniformities, which cause shorter-wavelength pyrometer channels to give an erroneously-high temperature reading.

## VI. DISCUSSION

To resolve the issue of why the measured temperatures are too high above 25 GPa, IR imaging experiments using the same experimental setup and samples prepared in the same way and made of the same material are desirable. These experiments, which can also quantify the percentage of surface area at higher radiance as well as the radiance (temperature) of the hot-spots, were conducted and they confirmed the occurrence of hot-spots. The temperatures of the hot-spots and their fractional areas of the surfaces appear to be in good agreement with estimates obtained from the free-surface temperature at different wavelengths, assuming a simple two-temperature model [35].

Results of these IR imaging experiments will be presented in a separate paper, currently in preparation [37].

The expected constant free-surface temperature of 505 K over a wide range of pressures was calculated assuming thermal equilibrium as well as a supported shock. Since the process of thermal transport takes a considerable amount of time (tens of nanoseconds to microseconds) and since our experimental approach of using direct HE drive produced Taylor waves [25], rather than a supported shock, a final determination of this plateau needs more experimental work. Furthermore, the departure of dynamic experiments from thermal equilibrium merits resolution.

### Acknowledgments

We would like to thank C. W. Greeff, D. B. Hayes and R. S. Hixson for valuable discussion in the planning stage of the experiments. The work was performed under the auspices of the US Department of Energy under Contracts W-7405-ENG-36 and DE-AC52-06NA25396.

[1] M. B. Zellner, M. Grover, J. E. Hammerberg, R. S. Hixson, A. J. Iverson, G. S. Macrum, K. B. Morley, A. W.

Obst, R. T. Olson, J. R. Payton, et al., Journ. Appl. Phys. **102**, 013522 (2007).
[2] M. B. Zellner, W. V. McNeil, J. E. Hammerberg, R. S. Hixson, A. W. Obst, R. T. Olson, J. R. Payton, P. A. Rigg, N. Routley, G. D. Stevens, et al., Journ. Appl. Phys. **103**, 123502 (2008).
[3] W. S. Vogan, W. W. Anderson, M. Grover, J. E. Hammerberg, N. S. P. King, S. K. Lamoreaux, G. Macrum, K. B. Morley, P. A. Rigg, G. D. Stevens, et al., Journ. Appl. Phys. **98**, 113508 (2005).
[4] S. S. Lutz, W. D. T. and; P. M. Rightley, and L. E. Primas, in *Proceedings of 12th Biennial International Conference of the APS Topical Group on Shock Compression of Condensed Matter* (2001).
[5] C. W. McCluskey, M. D. Wilke, W. D. Turley, G. D. Stevens, and L. R. Veeser, in *Proceedings of 26th International Congress on High-Speed Photography and Photonics*, edited by D. L. Paisley, S. Kleinfelder, D. R. Snyder, and B. J. THompson (SPIE, Bellingham, WA, 2005, 2004), vol. 5580, pp. 466–476.
[6] A. Seifter, M. Grover, D. B. Holtkamp, J. R. Payton, and P. Rodriguez, in *Proceedings of 26th International Congress on High-Speed Photography and Photonics*, edited by D. L. Paisley, S. Kleinfelder, D. R. Snyder, and B. J. THompson (SPIE, Bellingham, WA, 2005, 2003), vol. 5580, pp. 93–105.
[7] D. Partouche-Sebban, in *Proceedings of Shock Compression of Condensed Matter*, edited by M. D. Furnish, Y. M. Gupta, and J. W. Forbes (2004).
[8] V. W. Yuan, J. D. Bowman, D. J. Funk, G. L. Morgan, R. L. Rabie, C. E. Ragan, J. P. Quintana, and H. L. Stacy, Phys. Rev. Lett. **94**, 125504 (2005).
[9] R. L. Gustavsen and Y. M. Gupta, Journ. Appl. Phys. **75**, 2837 (1994).
[10] C. W. Greeff, Private communication (2005).
[11] C. W. Greeff, Tech. Rep. LA-UR-05-9414, Los Alamos National Laboratory (2005).
[12] J. D. Barnett, V. E. Bean, and H. T. Hall, Journ. App. Phys. **37**, 875 (1966).
[13] D. A. Young, *Phase Diagrams of the Elements* (University of California Press, Berkeley, 1991), pp. 106–107.
[14] D. B. Hayes, Private communication (2005).
[15] D. J. Steinberg, Tech. Rep. UCRL-MA-106439 change 1, Lawrence Livermore National Laboratory (1996).
[16] D. C. Swift, Private communication (2008).
[17] *Firing tank p/n 167-9818*, www.teledynerisi.com.
[18] K. Boboridis and A. W. Obst, in *Temperature: Its Measurement and Control in Science and Industry*, edited by D. Ripple (AIP, New York, 2003), vol. 7, p. 759.
[19] A. Seifter, K. Boboridis, J. Payton, and A. Obst, in *Proceedings of 26th International Congress on High-Speed Photography and Photonics*, edited by D. L. Paisley, S. Kleinfelder, D. R. Snyder, and B. J. THompson (SPIE, Bellingham, WA, 2005, 2003), vol. 5580, pp. 18–23.
[20] O. T. Strand, D. R. Goosman, C. Martinez, T. L. Whitworth, and W. W. Kuhlow, Rev. Sci. Instr. **77**, 083108 (2006).
[21] www.risi-usa.com/0products/1ebw/page23.html.
[22] P. Prevey and M. Mahoney, Materials Science Forum **4**, 2933 (2003).
[23] T. S. Migala and T. L. Jacobs, in *Surface Engineering: Coating and Heat Treatments* (2003), pp. 151–159.
[24] www.espi-metals.com.
[25] L. C. Mader, in *Symposium on high pressure* (1978).
[26] www.eritage.dupont.com.
[27] T. R. Gibbs and A. Popolato, *Los Alamos Series on Dynamic Material Properties* (University of California Press, Berkeley, 1980).
[28] D. C. Swift (2005).
[29] *Program and manuals for eul2d program* (2006), wessex Scientific and Technical Services Ltd., Perth.
[30] *Program and manuals for lagc1d program* (2006), wessex Scientific and Technical Services Ltd., Perth.
[31] D. B. Holtkamp, Private communication (2006).
[32] P. Herve, P. Masclet, A. Lefvre, I. Gobin, and J. P. Berthault, in *Proceedings of the 4th Symposium on temperature and thermal measurement in industry and science* (1990), p. 315.
[33] D. Partouche-Sebban, D. B. Holtkamp, R. R. Bartsch, H. Lee, and G. G. Schmitt, Rev. Sci. Instrum **72**, 3008 (2001).
[34] A. Seifter and D. C. Swift, Phys. Rev. B. **77**, 134104 (2008).
[35] A. Seifter and A. W. Obst, Int. Journ. Thermophys. **28**, 934 (2007).
[36] G. D. Stevens, S. S. Lutz, B. R. Marshall, W. D. Turley, L. R. Veeser, M. R. Furlanetto, R. S. Hixson, D. B. Holtkamp, B. J. Jensen, P. A. Rigg, et al., **104**, 013525 (2008).
[37] A. Seifter, in preparation.
[38] M. Grover, Private communication (2006).
[39] The radiance temperature $T_r$ is the temperature of a blackbody that emits the same radiance at a given wavelength as the object at temperature T. The radiance temperature $T_r$ is always lower than or equal to (in the case of a normal spectral emittance of 1) the true temperature T of an object.
[40] The pressures obtained by 2D simulations with simplified models of explosive initiation depend strongly on the assumed diameter for the detonator. The best match for the experimental data was achieved by assuming a ø 3mm detonator.
[41] These experiments were the first at STL for which the pressure needed to be preciselydetermined by changing the sample thickness. Later a more reproducible way to assemble the experimental setups was instituted, and recent results are more consistent. [38].
[42] Tensile stress for cavitation is much smaller than spall strength and cannot be seen in the PDV records.